# Lawrence Berkeley National Laboratory
**Recent Work**

**Title**
Dry Reforming of Methane on a Highly-Active Ni-CeO2 Catalyst: Effects of Metal-Support Interactions on C-H Bond Breaking.

**Authors**
Liu, Zongyuan
Grinter, David C
Lustemberg, Pablo G
et al.

Peer reviewed

# Dry Reforming of Methane on a Highly-Active Ni-CeO₂ Catalyst: Effects of Metal-Support Interactions on C-H bond breaking

Zongyuan Liu,[a] David C. Grinter,[b] Pablo G. Lustemberg,[c] Thuyduong Nguyen-Phan,[b] Yinghui Zhou,[d]  Si Luo,[a] Iradwikanari Waluyo,[b] Ethan J. Crumlin,[e] Dario J. Stacchiola,[b] Jing Zhou, [d] Javier Carrasco,[f] H. Fabio Busnengo,[c] M. Verónica Ganduglia-Pirovano,* [g] Sanjaya D. Senanayake,* [b] and José A. Rodriguez*[a,b]

**Abstract:** Ni-CeO₂ is a highly efficient, stable and non-expensive catalyst for methane dry reforming at relative low temperatures (700 K). The active phase of the catalyst consists of small nanoparticles of nickel dispersed on partially reduced ceria. Experiments of ambient pressure XPS indicate that methane dissociates on Ni/CeO₂ at temperatures as low as 300 K, generating CHₓ and COₓ species on the surface of the catalyst. Strong metal-support interactions activate Ni for the dissociation of methane. The results of density-functional calculations show a drop in the effective barrier for methane activation from 0.9 eV on Ni(111) to only 0.15 eV on Ni/CeO₂₋ₓ(111). At 700 K, under methane dry reforming conditions, no signals for adsorbed CHₓ or C species are detected in the C 1s XPS region.

[a]     BSc Z. Liu, BSc S. Luo, Prof J. A. Rodriguez
        Department of Chemistry, State University of New York
        Stony Brook, NY 11749 (USA)
        E-mail: rodrigez@bnl.gov
[b]     Dr D Grinter, Dr. T. Nguyen-Phan, Dr I. Waluyo, Dr D.J. Stacchiola,
        Dr J.A. Rodriguez, Dr S.D. Senanayake
        Chemistry Department, Brookhaven National Laboratory
        Upton, NY 11973 (USA)
        E-mail: ssenanay@bnl.gov
[c]     Dr P. G. Lustemberg, Prof H.F. Busnengo
        Instituto de Fisica Rosario (IFIR), CONICET - Universidad Nacional de Rosario (Argentina)
[d]     Dr Y. Zhou, Prof J. Zhou
        Department of Chemistry, University of Wyoming
        Laramie, Wyoming 82071 (USA)
[e]     Dr. Ethan J. Crumlin
        Advanced Light Source, Lawrence Berkeley National Laboratory,
        Berkeley, CA 94720 (USA)
[f]     Dr. Javier Carrasco
        CIC Energigune, Albert Einstein 48
        01510 Miñano, Álava (Spain)
[g]     Dr M.V. Ganduglia-Pirovano
        Instituto de Catálisis y Petroleoquímica, CSIC
        C/Marie Curie 2, 28049 Madrid (Spain)
        E-mail: vgp@icp.csic.es

XPS region. The reforming of methane proceeds in a clean and efficient way.

Methane and CO₂ are both common components of natural and land fill gas with great technological incentives to utilize both as reactants for the catalytic dry reforming process (CH₄ + CO₂ → 2CO + 2H₂, DRM).[1,2] A review of the scientific literature indicates that there are four key issues that must be addressed to optimize the DRM process for industrial applications: 1. Improve CH₄ activation; 2. Improve CO₂ activation; 3. Obtain a better understanding of the reaction mechanism for the formation of CO and H₂; and 4. Mitigate deactivation by carbon deposition.[1-3] The  DRM process likely involves the following series of sequential reactions: CH₄(g) → CH₄₋ₓ(a) + H(a) with x=1-4; CO₂(g)  → CO(a) + O(a); C(a) + O(a) → CO(g); H(a) + H(a) → H₂(g). The selective and stable conversion of CH₄ and CO₂ is challenging due to their high gas-phase stability. Generally, it is accepted that the DRM process is limited primarily by the activation of C-H bonds.[1,4,5] Noble metals (Pt, Ru, Rh, Pd), although highly active for this reaction, at high temperatures suffer from rapid deactivation through particle sintering and chemical poisoning (C or O deposition).[1-4] Due to its low cost, Ni dispersed on oxides is an attractive option as a catalyst for the DRM process.[1,6,7] Its use can be problematic due to a high temperature of operation or deactivation by carbon deposition/encapsulation.[7-9] In this work, we report the behavior of a highly efficient, stable and inexpensive Ni-CeO₂ catalyst for methane dry reforming at relatively low temperature (700 K). Strong metal-support interactions activate Ni for the dissociation of methane at a temperature as low as 300 K.

We prepared a NiO-CeO₂ mixed metal oxide catalyst and tested it for the  DRM process. Figure 1a displays an image of



NiO-CeO₂ precursor

transmission electron microscopy (TEM) for the as-prepared catalyst. It contained very small particles of NiO dispersed on a solid solution of Ce$_{1-x}$Ni$_x$O$_{2-y}$. The overall composition of the system was 20%-NiO/80%-CeO₂. The NiO-CeO₂ precursor was activated by exposing it to a stream of 20%H₂/He at 723 K. *In situ* measurements with time-resolved X-ray diffraction (Figure S1) showed a transformation of NiO into Ni⁰ and a minor expansion of the ceria lattice as a result of partial reduction. Figure 1b shows data for the DRM process on this Ni-ceria system. After exposure of the catalyst to the reactants, a steady-state is reached and the production of $CO_2$ and $H_2$ remains essentially constant after 80 hours of operation. The total conversion was ~ 12%, a value close to the expected thermodynamic limit at a temperature of 723 K.[1a] The results of *in situ* X-ray diffraction indicated that the active phase of the catalyst contained small nanoparticles of Ni dispersed on partially reduced ceria. TEM images for the used catalyst showed a negliglibe amount of carbon on the surface.

In order to understand better the chemistry of the DRM process on a nickel-ceria catalyst, we used ambient-pressure X-ray photoelectron spectroscopy (XPS) to study the interaction of $CH_4$, $CO_2$ and a $CH_4$/$CO_2$ mixture with model Ni/CeO₂(111) surfaces. Figure 2 shows images of scanning tunneling microscopy (STM) collected after depositing 0.1 ML of nickel on a CeO₂(111) film at 300 K with subsequent annealing to 500 K. At 300 K, there is a large dispersion of Ni on ceria with small particles that have an average height of 0.23 nm and an average diameter of 1.80 nm. XPS indicated that most of the nickel was in a 2+ oxidation state.[10,11] Annealing to 500 K induced some sintering of the Ni particles and large fraction of the Ni migrated into the ceria substrate to form a Ce$_{1-x}$Ni$_x$O$_{2-y}$ solid solution.[12,13]
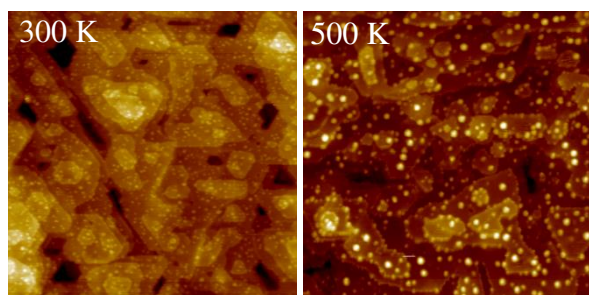


**Figure 2.** STM images for 0.1 ML Ni on CeO₂(111) after deposition at 300 K and annealing to 500 K. The area covered by each image is 120 nm x 120 nm.

Figure 3 shows a series of XPS spectra collected for a Ni/CeO₂(111) surface under 100 mTorr of methane. In the C 1s region, at 300 K, one sees a sharp peak for gaseous methane near 287 eV, a strong peak near 290.2 eV that can be attributed to adsorbed $CO_x$ species,[14] and weak features at 285-286 eV that probably come from $CH_x$ on the surface. This result implies that methane dissociates on the Ni/CeO₂ surface at room temperature. Some of the $CH_4$ molecules fully dissociate producing C atoms that eventually react with oxygen atoms of the ceria to yield $CO_x$ species. In the corresponding spectrum for the Ce 4d and Ni 3p regions no sign is evident for a change in the oxidation state of Ce⁴⁺ and Ni²⁺ cations. At 700 K, no features for $CO_x$ or $CH_x$ are seen in the in the C 1s region, but a clear change is seen in the line shape of the Ce 4d region (formation of Ce³⁺) and on the position of the Ni 3p peaks (Ni²⁺ → Ni⁰ transformation). We also detected the evolution of CO into gas phase during the exposure to $CH_4$ at this elevated temperature (Figure S2). Thus, there is a very fast reduction of the surface by methane. Once the first hydrogen is removed from the reactant molecule, a quick $CH_3$ → $CH_2$ → $CH$ → $C$

transformation occurs on the surface and the deposited carbon reacts with oxygen atoms of the sample to yield gaseous CO. The H atoms abstracted from the reactant desorb as $H_2$ or $H_2O$.
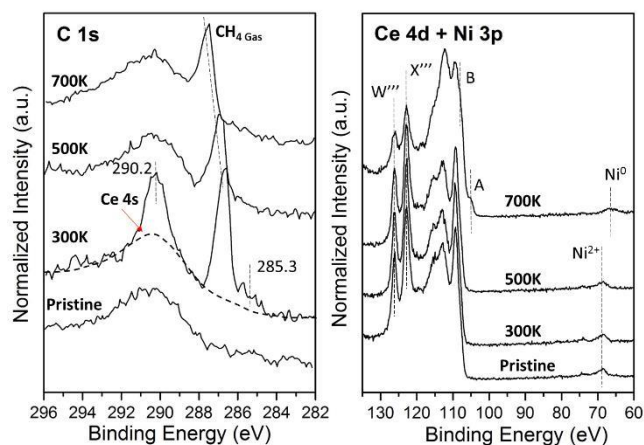


**Figure 3.** C 1s and Ce 4d + Ni 3p spectra of the Ni/CeO₂(111) ($\Theta_{Ni} \approx 0.1$ ML) surface under 100 mTorr of $CH_4$ at 300, 500 and 700 K.

We did similar experiments for a plain CeO₂(111) surface observing some reduction of the system but the amount of Ce³⁺ formed at temperatures above 600 K was much smaller than that on a Ni/CeO₂(111) surface under similar conditions, as seen in Figure 4. Thus, the addition of Ni to CeO₂ largely facilitates the interaction of the surface with methane.
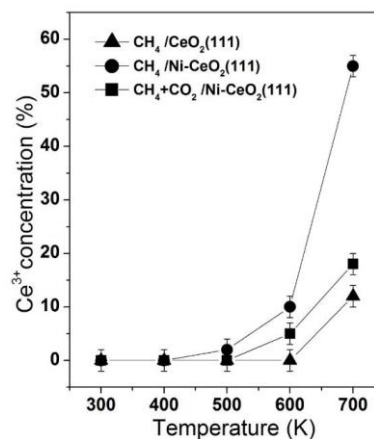


**Figure 4.** Ce³⁺ concentration measured in XPS as a function of temperature under reaction conditions (i.e. exposure to 100 mTorr of methane or a mixture of 100 mTorr of methane and 100 mTorr of $CO_2$).

Under a pressure of 100 mTorr of $CO_2$ at 300 K, the C 1s XPS spectrum for CeO₂(111) or Ni/CeO₂(111) surfaces exhibited a strong feature at 290.2 eV for an adsorbed $CO_x$ species.[14] This feature was seen at 300 K but essentially disappeared when the surfaces were heated to 500 or 700 K. Exposure to $CO_2$ did not induce any change in the oxidation state of the Ce⁴⁺ or Ni²⁺ cations. The addition of Ni to CeO₂(111) had a minor effect on the reactivity of the system towards $CO_2$. On the non-defective CeO₂(111) and Ni/CeO₂(111) surfaces we found no signs for the dissociation of the bonds of $CO_2$. The reactivity of these surfaces can be increased by the introduction of oxygen vacancies (Vac), $CO_2$(g) + Vac → CO(a) + O-Vac, or H adatoms,

$CO_2(g) + H(a) \rightarrow HOCO(a) \rightarrow HO(a) + CO(a)$. Both of them are present on a Ni/CeO$_2$(111) surface after exposing it to methane.

Figure 5 shows a set of XPS spectra collected for a Ni/CeO$_2$(111) catalyst under 100 mTorr of CH$_4$ and 100 mTorr of CO$_2$ at 300-700 K. At room temperature there was no catalytic activity, but at 700 K the formation of gaseous H$_2$ and CO was detected in a mass spectrometer. At 300 K, the C 1s region shows peaks for the gaseous reactants, CO$_2$ and CH$_4$, and features for adsorbed CO$_x$ and CH$_x$ species. A comparison with
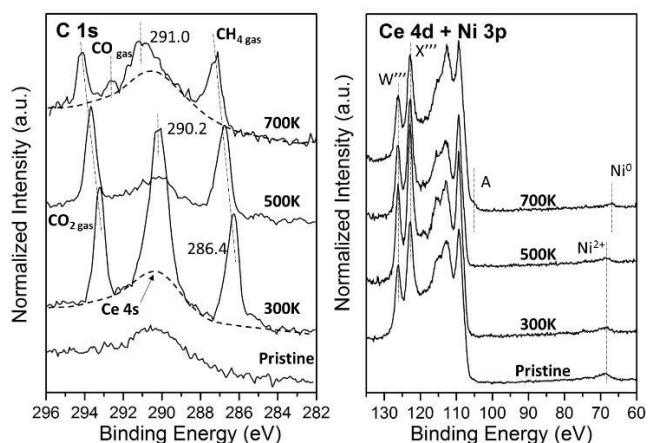


**Figure 5.** C 1s and Ce 4d + Ni 3p spectra of the Ni-CeO$_2$(111) ($\Theta_{Ni} \approx 0.1$ ML) surface under 100 mTorr CH$_4$ + 100 mTorr of CO$_2$ at 300, 500 and 700 K.

the XPS data in Figure 3 for exposure to only CH$_4$ points to an enhancement in the relative intensity of the signal for CO$_x$ probably as a consequence of the presence of CO$_2$ in the reactant feed. The signals for CO$_x$ and CH$_x$ disappear upon heating from 300 to 500 K. At 500 K, the surface of the catalyst contains Ni$^{2+}$ and Ce$^{4+}$ cations and no catalytic activity was observed. The system became catalytically active at 700 K, when the decomposition products of methane reduced Ni$^{2+}$ to Ni$^{0}$ and part of the Ce$^{4+}$ was transformed into Ce$^{3+}$. Thus, as observed in the *in-situ* XRD data for a powder catalyst (see above), the catalytically active phase contains small particles of metallic nickel on partially reduced ceria. In the C 1s spectrum at 700 K in Figure 5, in addition to the signals for the reactants, there are features for CO gas and a surface CO$_x$ species. The exact identity of this CO$_x$ species is difficult to assign precisely, due to variations in binding energy as a consequence of changes in work function and band bending with sample reduction, but it could be attributed to CO$_2^-$ or CO$_3^-$ species, stable on the surface thanks to the oxygen vacancies generated by the products of methane decomposition. The CO$_2$ present in gas phase reacts with the surface at 700 K and probably heals a significant fraction of the oxygen vacancies, $CO_2(g) + Vac \rightarrow CO(a) + O\text{-}Vac$. A deconvolution of the Ce 4d spectra in Figure 5 indicates that the net amount of Ce$^{3+}$ formed under a CH$_4$/CO$_2$ mixture is much smaller than under pure CH$_4$ (see a detailed comparison in Figure 4). Under a CH$_4$/CO$_2$ mixture, the C generated by the full decomposition of CH$_4$ does not react with O centers of the oxide, instead, it reacts with the O adatoms produced by the dissociation of CO$_2$.

An important point to notice in Figure 5 is the lack of signal for adsorbed elemental C or a nickel carbide on the surface. The nickel perturbed by a strong interaction with the ceria is able to dissociate methane but does not generate coke or carbon nanotubes, which is the typical behavior for bulk-like nickel.[8,9,15]

Methane decomposition is frequently cited as the most difficult step for the DRM process.[16] Here, we apply the spin-polarized DFT+U approach to investigate the dissociative adsorption of methane on Ni deposited on stoichiometric and reduced cerium oxide surfaces, plus the extended Ni(111) surface. The surfaces shown in Figure 2 are quite complex and very difficult to model. They evolve during reaction with part of the Ni sintering and other part migrating as single atoms into the bulk of ceria.[12,13] To model nickel in close contact with stoichiometric and reduced ceria, we have considered a quarter of a monolayer of Ni atoms deposited on CeO$_2$(111) and Ce$_2$O$_3$(0001) as ideal catalyst surfaces, aiming to elucidate the effects of the two supports in the Ni electronic and chemical properties towards CH$_4$ adsorption and dissociation as compared to Ni(111). Figures 6a and 6b show the Ni/ CeO$_2$(111) and Ni/Ce$_2$O$_3$(0001) structures, respectively. On CeO$_2$(111), the nickel oxidation state is 2+, while on Ce$_2$O$_3$(0001) is 0 (Figure S3). Metallic nickel is partially oxidized on the CeO$_2$(111) support, which is partially reduced.[17] However, on the reduced Ce$_2$O$_3$(0001) support, nickel remains metallic. Hence, these model surfaces mimic the essential features of the experimental catalysts as seen in the XPS data shown in Figures 3 and 5. The molecular binding of methane to Ni(111) is very weak and dissociation, CH$_4$(a) $\rightarrow$ CH$_3$(a) + H(a), is difficult due to a large energy barrier.[5,18] Our calculated barrier is ~0.9 eV (Figure 6), in agreement with many previous studies.[18] In contrast, supported Ni$^{2+}$ and Ni$^{0}$ atoms have an effective CH$_4$ dissociation barrier that is about 40% and 80% smaller than that for Ni(111), respectively. Therefore, the energy barriers of Ni supported on ceria are much more accesible at room temperature than that on Ni(111), in agreement with the experiments shown in Figures 3 and 5. Furthermore, we notice that chemisorbed CH$_4$ molecules are 0.35 eV more stable on Ni$^{0}$ than Ni$^{2+}$ sites, which increases the probability for reaction on the Ni$^{0}$/CeO$_{2-x}$ surfaces.
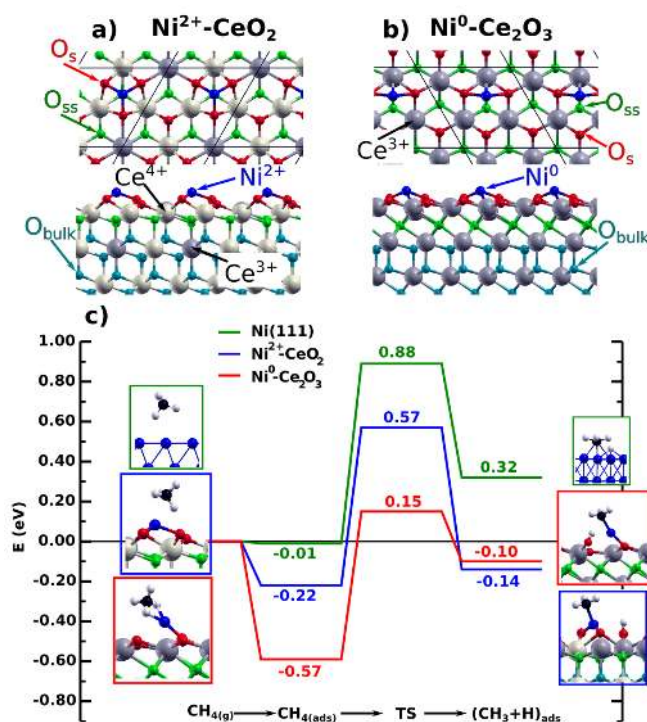


**Figure 6.** Atomic structure of Ni adsorbed on: a) CeO$_2$(111) and b) Ce$_2$O$_3$(0001). c) Reaction energy profile for the CH$_4$ $\rightarrow$ CH$_3$+H reaction on Ni(111), Ni$^{2+}$/CeO$_2$(111), and Ni$^{0}$/Ce$_2$O$_3$(0001). The structures shown on the left and right of the reaction pathways correspond to the side views of the optimized initial (molecularly adsorbed) and final (dissociated) states used in the search of the transition state (Supporting Information, Figure S4). O$_s$, O$_{ss}$, and O$_{bulk}$ stand for surface, subsurface, and bulk oxygen atoms.

The dissociation products for Ni$^{2+}$/CeO$_2$(111) and Ni(111) as shown in Figure 6c, do not correspond to the lowest energy states of CH$_3$ and H bound to the ceria surfaces, but stable

chemisorbed states geometrically close to the corresponding transition state (TS), which we show in Figure S4. We found that Ni and O atoms work in a cooperative way to dissociate $CH_4$ molecules in accordance with previous theoretical works. For example, Y. H. Chin et al. have shown that O adatoms facilitate the dissociation of $CH_4$ on Pd nanoclusters with TS geometries that are similar to those found in this study.[19] Adsorption sites with adjacent Ni and O atoms exist in our catalysts since Ni forms solid solutions with ceria, $Ce_{1-x}Ni_xO_{2-y}$.[12,13] Once $CH_3$ is formed, sequential decomposition of this intermediate into C should occur very fast.[18] Indeed, after exposing $Ni/CeO_2(111)$ to $CH_4$ at 300 K, a $CO_x$ species is detected in XPS as a product of the reaction between the C deposited by $CH_4$ decomposition and O atoms present in the catalyst surface (Figure 3).

Through strong metal-support interactions, oxides can activate and modify the electronic or chemical properties of a metal.[20,21] Strong metal-support interactions play a key role in the catalytic properties of $Ni/CeO_2$.[11,12] They enhance the reactivity of Ni towards methane dissociation and probably prevent the deposition of carbon and deactivation during the DRM process. As a result of these interactions, $Ni-CeO_2$ is a highly efficient, stable and inexpensive catalyst for methane dry reforming at relative low temperatures (700 K).

## Experimental Section

The $NiO-CeO_2$ powder precursor was prepared following the methodology described in ref. [22]. Upon characterization it was found that it contained small particles of NiO dispersed on a solid solution of Ni in ceria. The images of TEM for the $NiO-CeO_2$ precursor were acquired at the Center for Functional Nanomaterials at Brookhaven National Laboratory (BNL). The in-situ experiments with time-resolved X-ray diffraction were done at beamline X7B ($\lambda=0.3196$ Å) of the National Synchrotron Light Source at BNL. The sample was loaded into a silica capillary (0.9 mm ID, 1.0 mm OD) mounted on a flow system. $H_2$ in He was used to pretreat the $NiO-CeO_2$ precursor at 450 °C for 1 hr.. A 10 cc/min flow rate containing 20% $CO_2$, 20% $CH_4$, and 60% He was used to achieve 1:1 $CO_2/CH_4$ molar ratio.

To generate the films used to prepare the $Ni/CeO_2(111)$ model catalysts, Ce metal was evaporated onto a Ru single crystal (0001) held at 700 K in the presence of $5 \times 10^{-7}$ Torr $O_2$, and then annealed to 800 K for 10 mins at the same $O_2$ pressure.[12] The ceria films were estimated to be ca. 4 nm thick (~10 layers of O-Ce-O) based on the attenuation of the Ru 3d XPS signal with 650 eV incident photo energy, which can eliminate the interference of Ru $3d_{3/2}$ (284.0 eV) to the C 1s signal. Ni was vapor deposited on the as-prepared ceria film at 300 K under vacuum and then annealed to 700 K for 1 min.[12] The deposition rate of Ni was ~0.15 mono layer (ML) /min and the Ni coverages presented in this work are estimated to be 0.1-0.15 ML. The AP-XPS studies with the $Ni/CeO_2(111)$ catalysts were performed at the Advanced Light Source in Berkeley, CA (beamline 9.3.2). A VG Scienta R4000 HiPP analyzer was used for XPS analysis. The O 1s region was probed with photon energy of 650 eV, and the C 1s, Ni 3p, and Ce 4d regions with photon energy of 490 eV and a resolution of ~0.2 eV. The Ce 4d photoemission lines were used for binding energy calibration based on the 122.8 eV satellite features.

## Theoretical Section

The spin-polarized calculations were performed using the DFT-(PBE)+U approach as implemented in the Vienna ab initio simulation package (VASP){ vasp site, http://www.vasp.at; version vasp.5.3.5}. A value of 4.5 eV was used for the Hubbard U-like term. Dispersive interactions were not included. The projector augmented wave method (PAW) was used at a plane-wave cutoff of 415 eV to decouple the core from valence electrons. The C (2s, 2p), O (2s, 2p), Ni (3p, 3d, 4s), and Ce (4f, 5s, 5p, 5d, 6s) electrons were treated as valence states.

The $Ni/CeO_2(111)$ and $Ni/Ce_2O_3(0001)$ surfaces were modeled by (2 x 2) unit cells, with calculated ceria bulk equilibrium lattice parameters [$a_0=5.485$ Å ($CeO_2$); $a_0/c_0=3.92/6.18$ Å and internal parameters $uCe/uO=0.2471/0.6448$ (A-type $Ce_2O_3$)].. In the case of $CeO_2(111)$ we have considered nine atomic layers (three O-Ce-O trilayers) whereas

$Ce_2O_3(0001)$ was modeled with fifteen atomic layers (six Ce atomic layers). The Ni(111) surface was modeled by (3 x 3) unit cell (bulk lattice constant of 3.52 Å) and five Ni layers. In the three surface models, consecutive slabs were separated by at least 12 Å of vacuum space to avoid interaction with periodic images. Monkhorst-Pack grids with a (3 x 3 x 1) and (5 x 5 x 1) k-point sampling were used for the ceria-based systems and Ni(111) surface, respectively. All the atoms in the three bottom layers were fixed at their optimized bulk-truncated positions during geometry optimization, whereas the rest of the atoms were allowed to fully relax.

To locate the TS structures we employed the climbing image nudged elastic band method (CI-NEB)[23] with nine images for each reaction pathway. For all the TS reported in this work, we have found only one imaginary frequency, and the full geometry optimizations starting from its back and forward nearest configurations (along the reaction path) ended in a non-dissociated and dissociated state.

[1] a) D. Pakhare, J.Y. Spivey, *Chem. Soc. Rev.,* **2014**, *43*, 7813- 7837; b) R.Horn, R. Schlogl, *Catal. Lett.* **2015**, *145*, 23-39

[2] Y.H. Hu, E. Ruckenstein, *Adv. Catal.,* **2004**, *48*, 297-345.

[3] J.-M. Lavoie, *Frontiers in Chemistry,* **2014**, *2*, 81.

[4] R.H. Crabtree, *Chem. Rev.* **1995**, *95* (4), 987-1007.

[5] T. Choudhary, D.W.Goodman, *J. Mol. Catal. A-Chem.* **2000**, *163*, 9-18.

[6] K. Mette, S. Kühl, H. Düdder, K. Kähler, A. Tarasov, M. Muhler, M. Behrens, *ChemCatChem*, **2014**, *6*, 100-104.

[7] X. Du, D. Zhang, L. Shi, R. Gao, J. Zhang, *J. Phys. Chem. C*, **2012**, *116*, 10009-10016

[8] B. Steinhauer, M.R. Kasireddy, J. Radnik, A. Martin, *Applied Catal. A-General* **2009**, *366*, 333-341.

[9] S.A. Theofanidis, V.V. Galvita, H. Poelman, G.B. Marin, *ACS Catal.* **2015**, *5*, 3028-3039.

[10] Y. Zhou, J. Zhou, *J. Phys. Chem. C*, **2012**, *116*, 9544-9549.

[11] J. Carrasco, D. López-Duran, Z. Liu, T. Dunchoň, J. Evans, S.D. Senanayake, E.J. Crumlin, V. Mantolin, J.A. Rodriguez, M.V. Ganduglia-Pirovano, *Angew. Chem. Int. Ed.* **2015**, *127*, 3989-3993.

[12] S. Senanayake, J. Evans, S. Agnoli, L. Barrio, T. Chen, J. Hrbek, J.A. Rodriguez, *Topics in Catalysis* **2011**, *54*, 34-41.

[13] a) A. Caballero, J.P. Holgado, V.M. Gonzalez-de la Cruz, S.E. Habas, T. Herranz, M. Salmeron, M. *Chem. Commun.* **2010**, *46*, 1097-1099; b) D. Kong, J. Zhu, K.-H. Ernst, *J. Phys. Chem. C*, **2016**, 5980-5987.

[14] K. Mudiyanselage, S.D. Senanayake, L. Feria, S. Kundu, A.E. Baber, J. Graciani, A.B. Vidal, S. Agnoli, J. Evans, R. Chang, S. Axnanda, Z. Liu, J.F. Sanz, P. Liu, J.A. Rodriguez, D.J. Stacchiola, *Angew. Chem. Int. Ed.* **2013**, *52*, 5101-5105.

[15] K. Otsuka, Y. Abe, N. Kanai, Y. Kobayashi, S. Takenaka, E. Tanabe, *Carbon*, **2004**, *42*, 727-736.

[16] J. Wei, E. Iglesia, *J. Phys. Chem. B*, **2004**, *108*, 4094-4103.

[17] J. Carrasco, L. Barrio, P. Liu, J. A. Rodriguez, M. V. Ganduglia-Pirovano, *J. Phys. Chem. C*, **2013**,*117*, 8241-8250.

[18] a) F. Abild-Pedersen, O. Lytken, J. Engbæk, G. Nielsen, I. Chorkendorff and J. K. Nørskov, *Surf. Sci.*, **2005**, *590*, 127-137; b) S. Nave, A.K. Tiwari and B. Jackson, *J. Chem. Phys.,* **2010**, 132, 054705:1-12; c) B. Jiang, R. Liu, J. Li, D. Xie, M. Yang and H. Guo, *Chem. Sci.,* **2013**, 4, 3249-3254; d) J. Li, E. Croiset and L. Ricardez-Sandoval, *Chem. Phys. Lett.,* **2015**, 639, 205–210.

[19] Y.H. Chin, C. Buda, M. Neurock, E. Iglesia *J. Am. Chem. Soc.* **2013**, *135*, 15425-15442.

[20] a) M. Sterrer, T. Risse, U. Martinez Pozzoni, L. Giordano, M. Heyde, H.-P. Rust, G. Pacchioni, H.-J. Freund, *Phys. Rev. Lett.* **2007**, *98*, 096107; b) A. Bruix, J. A. Rodriguez, P. J. Ramirez, S. D. Senanayake, J. Evans, J. B. Park, D. Stacchiola, P. Liu, J. Hrbek, F. Illas, *J. Am. Chem. Soc.* **2012**, *134*, 8968 – 8974; c) A. Bruix et al., *Angew. Chem. Int. Ed.* **2014**, *53*, 10525 – 10530; *Angew. Chem.* **2014**, *126*, 10693 – 10698; d) V. Simic-Milosevic, M. Heyde, N. Nilius, T. Konig, H.-P. Rust, M. Sterrer, T. Risse, H.-J. Freund, L. Giordano, G. Pacchioni, *J. Am. Chem. Soc.* **2008**, *130*, 7814 – 7815.

[21] a) T. Lunkenbein, J. Schumann, M. Behrens, R. Schlögl, M.G. Willinger, *Angew. Chem. Int. Ed.* **2015**, *54*, 4544-4548; b) J. Schumann, M. Eichelbaum, T. Lunkenbein, N. Thomas, M.C. Álvárez-Galvan, R. Schlögl, M Behrens, *ACS Catal.* **2015**, *5*, 3260-3270.

[22] a) G. Zhou, L. Barrio, S. Agnoli, S. D. Senanayake, J. Evans, A. Kubacka, M. Estrella, J. C. Hanson, A. Martínez-Arias, M. Fernández-García, J. A. Rodriguez, *Angew. Chem.* **2010**, *122*, 9874-9878; b) L. Barrio, A. Kubacka, G. Zhou, M. Estrella, A. Martínez-Arias, J. C. Hanson, M. Fernández-García, J. A. Rodriguez, *J. Phy. Chem. C*. **2010**, *114*, 12689-12697.

[23] G. Henkelman, B. P. Uberuaga, H. Jónsson, *J. Chem. Phys.* **2000**, 113, 9901 – 9904.

TOC

**Text for Table of Contents:**

Ni-CeO$_2$ is a highly efficient, stable and non-expensive catalyst for methane dry reforming at relative low temperatures (700 K). The active phase of the catalyst consists of small nanoparticles of nickel dispersed on partially reduced ceria. Experiments of ambient pressure XPS indicate that methane dissociates on Ni/CeO$_2$ at temperatures as low as 300 K, generating CH$_x$ and CO$_x$ species on the surface of the catalyst. Strong metal-support interactions activate Ni for the dissociation of methane.